NJC

Accepted Manuscript

This is an *Accepted Manuscript*, which has been through the Royal Society of Chemistry peer review process and has been accepted for publication.

Accepted Manuscripts are published online shortly after acceptance, before technical editing, formatting and proof reading. Using this free service, authors can make their results available to the community, in citable form, before we publish the edited article. We will replace this *Accepted Manuscript* with the edited and formatted *Advance Article* as soon as it is available.

You can find more information about *Accepted Manuscripts* in the Information for Authors.

Please note that technical editing may introduce minor changes to the text and/or graphics, which may alter content. The journal's standard Terms & Conditions and the Ethical guidelines still apply. In no event shall the Royal Society of Chemistry be held responsible for any errors or omissions in this *Accepted Manuscript* or any consequences arising from the use of any information it contains.

ROYAL SOCIETY OF CHEMISTRY

www.rsc.org/njc

Journal Name

RSCPublishing

ARTICLE

Valine-Derived Carbon Dots with Color-Tunable Fluorescence for High Sensitivity and Selectivity Detection of Hg^{2+}

Cite this: DOI: 10.1039/x0xx00000x

Received 00th January 2012,
Accepted 00th January 2012

DOI: 10.1039/x0xx00000x

www.rsc.org/

Chunfang Zhang, Zhongbo Hu, Li Song, Yanyan Cui*, and Xiangfeng Liu*

Hg^{2+} has been regarded as one of the most ubiquitous and dangerous pollutants for human health and environment. It is still of a great challenge to develop a simple and ultrasensitive method for aqueous Hg^{2+} detection. Carbon dots (CDs) have attracted great attention due to their potential applications in bioimaging, chemsensors and photocatalyst design. Herein, we report a simple and efficient method to prepare P-doped carbon dots (CDs) with tuneable fluorescence colours using L-valine as the carbon sources and H_3PO_4 (85%) as the oxidant. The fluorescent colour of CDs can be feasibly tuned from green (CDs-1) to yellow (CDs-2) through simply controlling the reaction time under a mild temperature (90°C). The obtained CDs possess bright photoluminescence with quantum yield (QY) up to 44.8% for CDs-1 and 31% for CDs-2, excellent biocompatibility and water solubility. The fluorescence intensity of CDs-1 also is sensitive to pH. More importantly, the green CDs show high sensitivity and selectivity for the detection of Hg^{2+}.Two different fluorescence quenching modes are discovered and the lower limit of detection (LOD) is about 1.51 nM.

1. Introduction

Mercury ion is one of the most toxic heavy metals ion and has been regarded as one of the most ubiquitous and dangerous pollutants for human health and environment[1-4]. It has been revealed that the exposure to high concentrations of mercury ion can induce a serious of toxicological effects for human health such as brain damage, central nervous system damage, endocrine system damage, various cognitive and motion disorders[2,4]. There is a growing demand to develop a rapid and user-friendly method for the sensitive and selective detection of Hg^{2+} ion [2]. Up to now, a few methods for tracking Hg^{2+} have been reported such as atomic absorption spectrometry, atomic fluorescence spectrometry (AAS), inductively coupled plasma mass spectrometry (ICP-MS), selective cold vapour atomic fluorescence spectrometry and electrochemical methods[5,6], and so forth. However, these instrumental techniques not only require sophisticated instruments but also complicated sample preparation processes, which limit the practical applications in routine Hg^{2+} detection[7,8]. Therefore, it is still of a great challenge to develop a simple method for aqueous Hg^{2+} detection. To solve these problems, a variety of sensors have been developed and used for the detection of Hg^{2+} [2]. Nevertheless, the poor selectivity, low resolution in aqueous media, insufficient sensitivity, expensive instrumentation, and/or the complex preparation procedure of the probe materials restrict the practical use of the above mentioned sensors [3,8,9]. In contrast, fluorescent sensors offered a simple, rapid and low-cost approach for tracking metal ions in the biological and environmental samples [9]. Quantum dots (QDs) with the high fluorescence quantum yield and size-tuneable emission profile have been considered as one of the most promising optical sensing nanomaterials for the detection of metal ions [2,10]. However, the traditional QDs show poor solubility in water and high toxicity at relatively low concentrations, which largely restrict their analytical potential [11,12].

Fluorescent carbon dots (CDs) with broad excitation spectra and tuneable emission spectra are regarded as the next generation fluorescent nanomaterials and the promising alternatives to the conventional luminescent semiconductor quantum dots composed of toxic heavy metals such as Cd^{2+} [13-16]. As a new class of fluorescent nanomaterials with the sizes below 10 nm, CDs have drawn considerable attention in a wide variety of biomedical fields, such as biosensor [15,17,18], bioimaging [19], drug delivery [20,21] and gene delivery [22,23]. Recently, CDs have been actively applied in biosensing and a few scientific papers about mercury ions and biological molecules sensing based on CDs have been reported [2,24].

CDs were discovered serendipitously by researchers purifying single walled carbon nanotubes fabricated by arc-discharge methods [25] and several approaches have been developed for synthesizing CDs including chemical and physical methods [20,26]. Chemical methods include electrochemical synthesis [27], microwave methods[28], thermal oxidation treatment [29], hydrothermal or acidic oxidation [30], ultrasonic routes [31], carbonisation of carbohydrates [32,33], and so on. Physical methods include arc discharge[34], laser ablation of graphite [35], and plasma treatment[36]. Among of these methods, acidic oxidation has been proved to be an effective and convenient way to synthesize CDs with sufficient fluorescence quantum yield (QY) without requiring elaborate apparatus .[37]

In this study, we report a simple, economical and green method for the synthesis of water-soluble and phosphorus functionalized CDs with QY of 44% and tuneable luminescence. In this process, L-valine is served as the carbon source for the first time with phosphoric acid as the oxidation agent. The fluorescent colour of CDs can be feasibly tuned from green to yellow by just changing the

reaction time under a mild temperature (90°C). The obtained CDs were readily soluble in water to form a stable, yellowish, and transparent aqueous solution without precipitation for a few months. More importantly, the CDs show high sensitivity and selectivity for the detection of Hg^{2+}. Two different fluorescence quenching modes are discovered and the lower limit of detection (LOD) is 1.51 nM.

2. Experimental section

2.1 Materials

L-valine was purchased from Japan and all other chemicals were purchased from Sigma-Aldrich. All glassware was washed with aqua regia (conc. HCl: conc. HNO_3, volume ratio = 3:1), and then rinsed with ultrapure water and ethanol. The water used throughout all the experiments was purified through a Millipore system.

2.2 Synthesis of CDs

The general method for the synthesis of the CDs was as follows: the both CDs were synthesized by mixing 1 mL of aqueous L-valine solution (100 mg/mL) with 2 mL of concentrated phosphoric acid and heating the solution at 90°C for 4～10 h. For example, 1 mL of aqueous L-valine solution (100 mg/mL) with 2 mL of concentrated phosphoric acid and heating the solution at 90 °C for 4 h to obtain the CDs-1. Similarly, 1 mL of aqueous L-valine solution (100 mg/mL) with 2 mL of concentrated phosphoric acid and heating the solution at 90 °C for 10 h to obtain CDs-2. The synthesized brown solution was neutralized with 1 M NaOH solution (The pH value was about 7) and filtered with a 0.22 μm polyethersulfone (PES) membrane to discard the possible large and insoluble particles. The obtained CDs were further purified by dialyzing against deionized water using a membrane with dialysis membrane (molecular weight cut-off = 500) for 7 h to obtain the final CDs.

2.3 Characterizations

UV−vis spectra were obtained on a UV5800 spectrophotometer. X-ray photoelectron spectroscopy (XPS) analysis was measured on an ESCALAB MK II X-ray photoelectron spectrometer using Mg as the exciting source. FTIR spectrum was measured on an IFS 66V/S (Bruker) IR spectrometer in the range of 1000 – 1500 cm^{-1}. High resolution transmission electron microscopy (HRTEM) measurements were made on JEM-1200EX electron microscopy with an accelerating voltage of 100 kV. The sample for TEM characterization was prepared by placing a drop of colloidal solution on carbon-coated copper grid and dried at room temperature. Fluorescent emission spectra were recorded on a RF-5301PC spectrofluorometer (Shimadzu, Japan). QY was measured choosing rhodamine 6G in Ethanol (literature quantum yield 0.95 at 488 nm) as a standard for CDs. The optical densities measured on UV−vis spectra were obtained on a UV5800 spectrophotometer. Absolute values are calculated using the standard reference sample that has a fixed and known fluorescence QY value.

2.4 Quantum yield

The QY of these CDs was calculated by measuring the fluorescence intensity in aqueous dispersion by using the following equation,

$$Q_{CD} = Q_R \bullet \frac{I_{CD}}{I_R} \bullet \frac{A_R}{A_{CD}}$$

where Q is the quantum yield, I is the measured intensity of luminescent spectra, A is the optical density at exited wavelength. QY was measured choosing rhodamine 6G in Ethanol (literature quantum yield 0.95 at 488 nm) as a standard for CDs. The subscript ''R'' refers to standard with known quantum yield and ''CD'' for the sample in this equation. In order to minimize reabsorption effects, absorbencies in the 10 mm fluorescence cuvette were kept under 0.05 at the excitation wavelength (363 nm).

2.5 Effect of metal ions, pH and NaCl solution on the PL of CDs-1

To the best of our knowledge, there usually co-exist some common metal ions in urine and pharmaceutical preparations. To address the question whether foreign coexisting substance imply effect on the measurement of the CDs-1 or not, further interference experiments were performed in the presence of the CDs-1 (2 mg/mL) together with common metal ions. For the detection of various metal ions, the aqueous solutions of Hg^{2+}, Ca^{2+}, Ba^{2+}, Cu^{2+}, Co^{2+}, Fe^{3+}, Mn^{2+}, Mg^{2+}, Ni^{2+}, K^+ , Na^+ (5 mM) were first prepared and used as different metal ion sources. The PL spectra of CDs in the absence and presence of various metal ions were recorded under a 363 nm excitation. In addition, the green CDs were added into deionized water with different pH values and NaCl solution (1 M). The corresponding PL spectra of the CDs-1 were then obtained under excitation at 363 nm.

2.6 Sensitive detection of Hg^{2+} ion

The sensitivity detection of Hg^{2+} ions was executed at room temperature in aqueous solution. A serious of Hg^{2+} aqueous solutions with various concentrations were freshly prepared before use. To evaluate the sensitivity to Hg^{2+}, Hg^{2+} aqueous solutions with various concentrations were added into CDs aqueous solution. Then the quenching effects of Hg^{2+} on the fluorescence density of the CDs were examined. The PL spectra were recorded by the fluorescence spectrophotometer with an excitation wavelength of 363 nm.

3. Results and discussions

3.1 Synthesis of C-dots

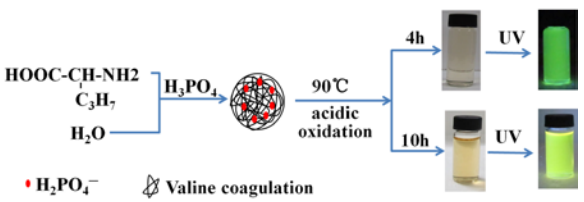

Scheme. 1 Schematic representation of the synthesis process and mechanism of the phosphate functionalized CDs-1 and CDs-2.

The synthetic process is demonstrated in Scheme. 1. According to the previous studies on the formation mechanism of CDs from small molecules, we hypothesise that the formation mechanism is as follows (Scheme. 1): (1) hydrolysis of L-valine and coagulation with phosphoric acid; (2) polymerization of the coagulated L-valine at a higher temperature; (3) nucleation and growth of carbon substances formed in the previous step; (4) oxidation of the grown carbon substances and phosphate functionalization [20,38]. The emission colour

of CDs might be largely influenced by size, shape, and composition-related factors, such as P-doping, content of sp^2 carbon and surface defects [25,39-43].

3.2 The photoluminescence properties of CDs

The optical properties of the CDs-1 and CDs-2 are shown in Fig. 1. As shown in the UV–vis absorption spectra (Fig. 1A and Fig. 1B), both CDs show two apparent absorption peaks: (1) a peak at 223 nm (CDs-1) and 224 nm (CDs-2), which is due to the n→ p* transition of C=O bond and (2) a weaker peak at 269 nm (CDs-1 and CDs-2), which can be attributed to the $\pi \rightarrow \pi^*$ transition of aromatic sp^2 bond [20,44]. The PL spectra of the two CDs are shown in Fig. 1C ~ F, it can be seen that CDs-1 show a strong PL at 521 nm when they are excited at 363 nm while CDs-2 display an obvious PL at 574 nm excited at 412 nm. Using rhodamine 6G (QY = 0.95 in ethanol) as a reference, the QY of the CDs in water is determined to be 44.8% for CDs-1 and 31% for CDs-2, which is comparable to previous reports [20,30]. As shown in the insets of Schem. 1, CDs-1 emits green PL and CDs-2 emits yellow PL under UV radiation of 365 nm. Interestingly, the emission from CDs-1 only shift about 10 nm but the emission from CDs-2 shifts about 30 nm with excitation wavelength (λ_{ex}) (Fig. 1C and D). The λ_{ex} dependent PL behaviour is common in CDs.

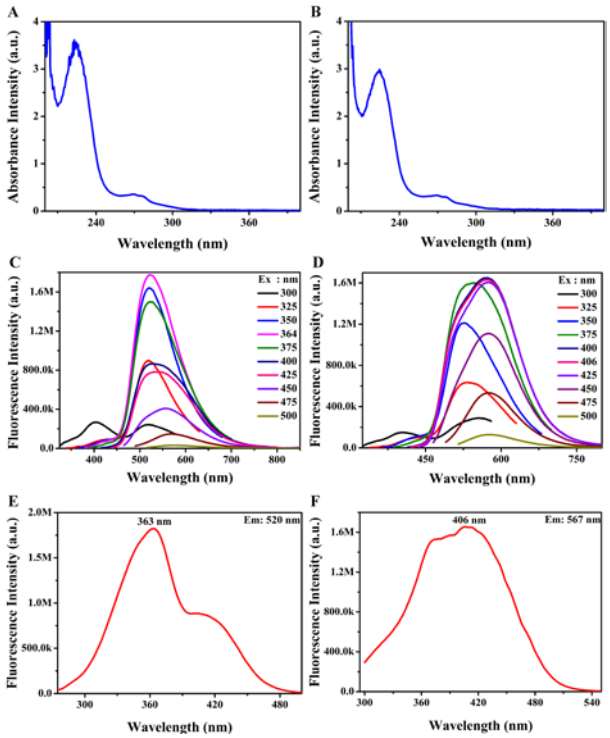

Fig. 1 Absorption spectra of the CDs-1 (A) and CDs-2 (B) and Emission spectra of CDs-1 (C) and CDs-2 (D). Excitation spectra of the CDs-1 (E) and the CDs-2 (F)

3.3 Characterization of CDs

The size and morphology of both CDs-1 and the CDs-2 were observed by high resolution transmission electron microscope (HRTEM) (Fig. 2). The CDs-1 shown in the Fig. 2A was well dispersed quasi-spherical nano-dots within the range of 1~3 nm in size. The HRTEM image of CDs-1 shows a lattice spacing of 0.18 nm, which is close to the [102] facet of graphite carbon [9]. Meanwhile, HRTEM image of CDs-2 in Fig. 2B demonstrates that the size distribution of CDs-2 is 2~4 nm. In addition, the HRTEM image also indicated that CDs-2 possess a crystalline structure consisting of parallel crystal planes with a lattice of 0.31 nm, which is close to that of phosphorus-doped carbon quantum dots (0.3 nm) [45]. A previous study has proved the relationship between the energy gap and particle size, which indicated that the energy gap gradually decreased with the increase of particle size [46]. Therefore, the different emission features of the obtained CDs might be largely attributed to the size effect.

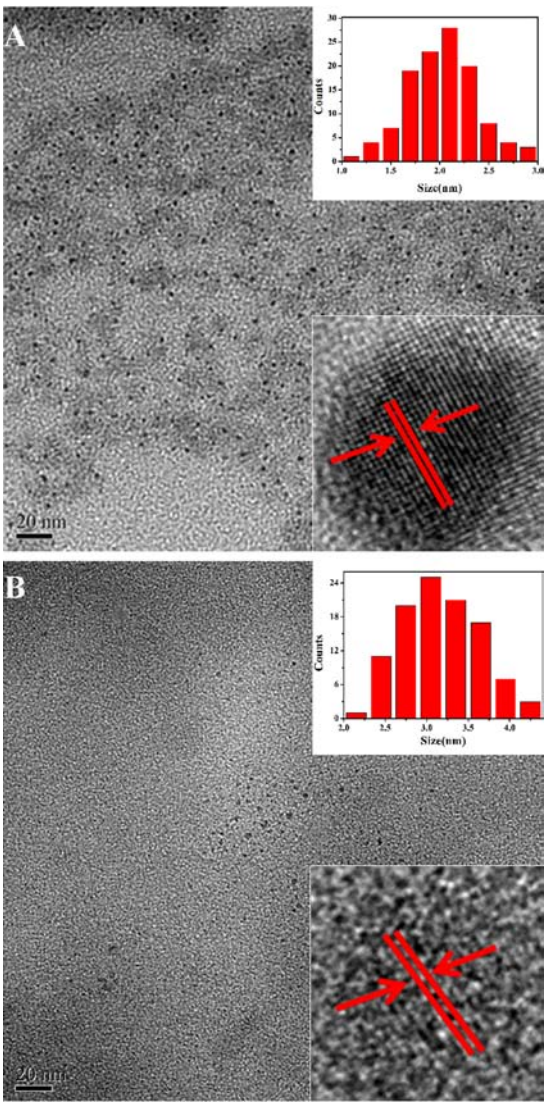

Fig. 2 HR-TEM images of the CDs-1 (A) and CDs-2 (B), the insets show the particle size distribution of CDs.

The composition of the CDs-1 and CDs-2 were characterized by X-ray photoelectron spectroscopy (XPS) (Fig. 3). As seen in Fig. 3A and B, the XPS survey of the both CDs exhibited four apparent peaks at around 282, 397, 530 and 131 eV, which can be attributed to C_{1s}, N_{1s}, O_{1s} and P_{2p}, respectively, which indicates that the obtained CDs are mainly composed of four elements of C, O, N and P. The contents of C, O, N and P in the CDs-1 and CDs-2 are summarized in Table 1. The contents of C, O, N and P in the CDs-1 are 42.88, 54.34, 1.27 and 1.51%, respectively. The C, O, N and P contents CDs-2 were 40.52%, 55.25%, 2.09% and 2.14%, respectively. More chemical information of the CDs-1 was

described in the C_{1s}, O_{1s}, N_{1s} and P_{2p} spectrum. The C_{1s} spectrum (Fig. 3C) can be fitted into two peaks at around 282.4 eV, which are attributed to C–C/C=C, C=O and C–O groups, respectively [2,41]. In the N_{1s} spectrum (Fig. 3E), the peak at around 397.5 eV can be ascribed to C–N–C/C=N groups [2]. From the O_{1s} spectrum shown in Fig. 3G, the peak at 529.6 eV can be assigned to C–O–C groups[47]. As shown in Fig. 3I, a P_{2p} spectrum displays a peak at 131.6 eV for P–O [48]. Meanwhile, the C_{1s}, O_{1s}, N_{1s} and P_{2p} spectrum of CDs-2 were also shown in Fig. 3. The C_{1s} spectrum (Fig. 3D) is similar to that of CDs-1 and can also assigned to three types of carbon bonds at around 282.8 eV, namely, C–C/C=C, C=O and C–O groups[2,41]. As for N_{1s} spectrum (Fig. 3F) the peak at around 397.7 eV could be ascribed to C=N/C-N-C, N-H and NO_2, respectively. The O_{1s} spectrum (Fig. 3H) can also be deconvoluted into two peaks: C-O-C and C=O at around 530.1 eV [2,47]. As shown in Fig. 3J, a deconvoluted P_{2p} spectrum displays two peaks at around 131.6 eV for P–O and P=O [48]. The comparison results indicated the higher doping concentration of phosphorus and higher oxidation state of CDs-2 than CDs-1, which might be partly responsible for the fluorescent red shift.

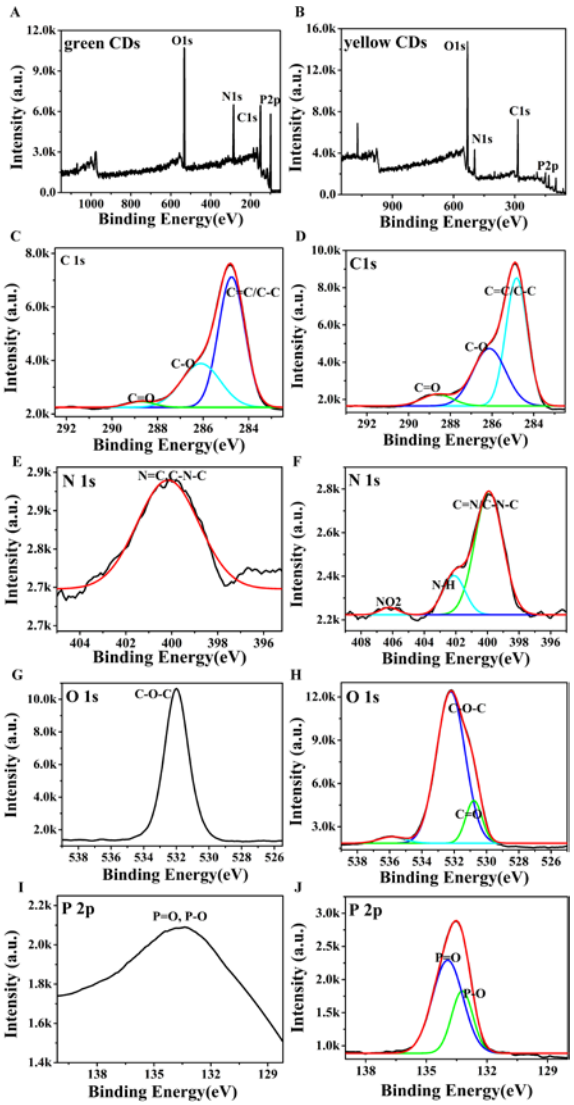

Fig. 3 XPS spectrum of CDs-1 (A) and CDs-2 (B). XPS spectra of C_{1s} (C), N_{1s} (E), O_{1s} (G) and P_{2p} (I) for CDs-1. XPS spectra of C_{1s} (D), N_{1s} (F), O_{1s} (H) and P_{2p} (J) spectrum CDs-2.

Table1. The contents of C, O, N and P in CDs-1 and CDs-2 determined by XPS.

	C Atomic/%	N Atomic/%	O Atomic/%	P Atomic/%
CDs-1	42.88	1.27	54.34	1.51
CDs-2	40.52	2.09	55.25	2.14

We also used the Fourier transform infrared spectroscopy (FTIR) to study the surface functional groups of the two CDs (Fig. 4). The FTIR spectra of the two CDs are similar. As shown in the Fig. 4, the spectrums revealed the existence of the signature of the Ar–O–P bond at ~1237 cm^{-1}, indicating the attachment of phosphate to the two CDs [48]. The functional groups analyzed by the FTIR are consistent with XPS. Moreover, the characterizations from HRTEM, FTIR and XPS indicated that phosphorus groups are successfully transferred from valine molecules to the CDs surface during the particle formation.

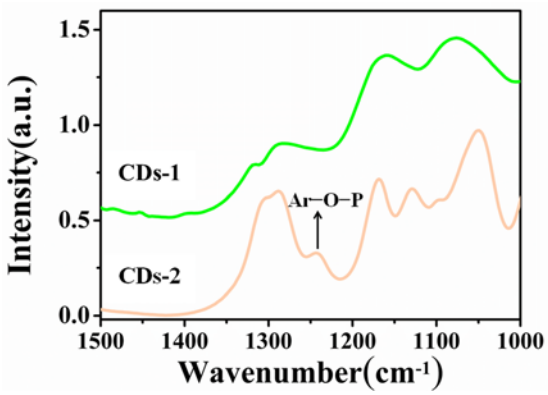

Fig. 4 FTIR spectra of CDs-1 and CDs-2.

3.4 Optical properties application of CDs-1

The optical properties of CDs-1 are further studied due to its higher QY. The influence of pH on the PL intensity of the CDs-1 was studied in the pH range of 3~11. As shown in Fig. 5A, the PL intensity obviously decreased at pH=5~8 and slightly increased at pH = 8~11. The pH-dependent behaviour might be largely attributed to variation of the surface chemical groups of the CDs-1 under different pH value. The detailed mechanism needs to be further studied. Moreover, the optical pH-sensitivity of the CDs-1 could be exploited for various biomedical applications, such as the diagnosis of tumour micro-environment[49,50]. The influence of NaCl (Fig. 5B) solution on the PL intensity of the CDs-1 was also examined. We found that the PL intensity did not significantly change with the addition of NaCl solution.

In addition, the effect of metal ions on the PL of the CDs-1 was evaluated by recording the PL intensities in the presence and absence of the 5 mM metal ions (Hg^{2+}, Ca^{2+}, Ba^{2+}, Cu^{2+}, Co^{2+}, K^{+}, Na^{+}, Fe^{3+}, Mn^{2+}, Mg^{2+}, and Ni^{2+}). The peak position of the maximum emission was not affected upon the addition of metal ion. Therefore, fluorescence intensity differences of the CDs-1 in the presence of different metal ions were plotted (Fig. 6A). Notably, the fluorescence intensity considerably decreased upon the addition of

Hg^{2+}. However, the addition of other metal ions does not significantly change fluorescence intensity, which indicates that the CDs-1 may be developed as a sensor for the detection of Hg^{2+}.

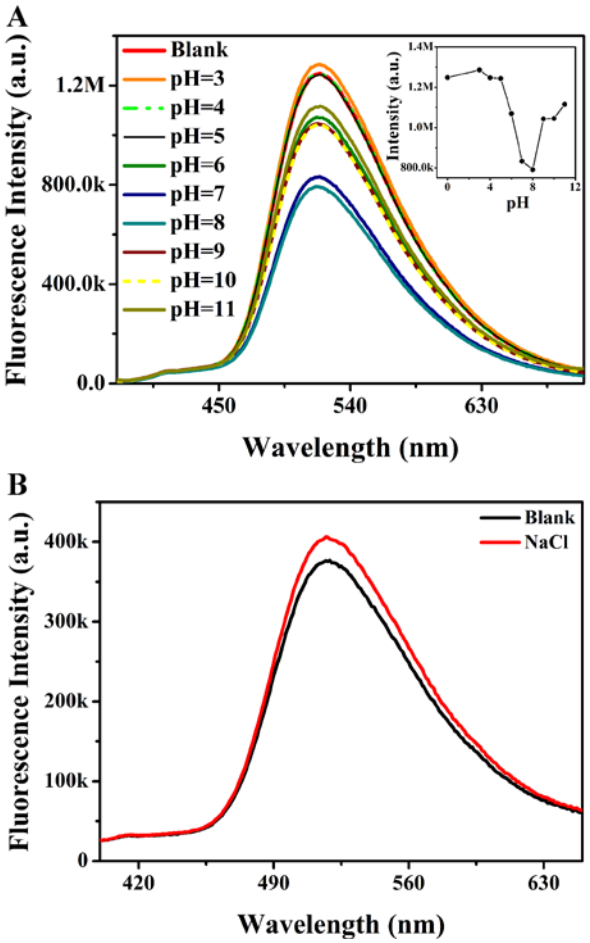

Fig. 5 (A) The influence of pH values on the PL intensity of the CDs-1. The inserted figure is to describe the dependence of the fluorescence intensity peak on pH. (B) The influence of 1M NaCl on the PL intensity of the CDs-1.

We further investigated the potential capability of CDs-1 for quantitative detection of Hg^{2+}. Different concentrations of Hg^{2+} were added to the aqueous solution of the CDs-1 and the fluorescence intensity was measured to evaluate the sensitivity of the CDs-1 chemosensor. As shown in Fig. 6B, the fluorescence intensity of the CDs-1 at 520 nm gradually decreases with increasing concentration of Hg^{2+} indicating that the addition of Hg^{2+} ions can effectively quench the fluorescence of the CDs-1. Fig. 6B presents the fluorescence intensity under different concentrations of Hg^{2+} ions. A good linear correlation (R^2=0.991) is exhibited over the concentration range of 0～10 nM and the limit of detection (LOD), which was defined as 3 times standard deviation/slope by the International Union of Pure and Applied Chemistry (IUPAC) standard, was calculated to be 1.51 nM. This is much lower than what's reported in the previous publications[2,8,9]. For example, Zhang et al[2] synthesized nitrogen-doped carbon quantum dots using folic acid and LOD for Hg^{2+} is about 0.23 μM. More interestingly, another good linear correlation (R^2=0.998) is also demonstrated over the concentration range of 100～5000 nM and the LOD was about 126 nM. The two linear correlations with different slopes might correspond to two different fluorescence quenching modes. Based on the previous reports, we speculate that when the molar amount of Hg^{2+} is much lower than the CDs the fluorescence quenching could be largely attributed to metallophilic interaction[51]. But with the increase of the Hg^{2+} concentration the Hg^{2+} may induce the CDs-CDs interaction and aggregation, and result in the fluorescence quenching [52-54].

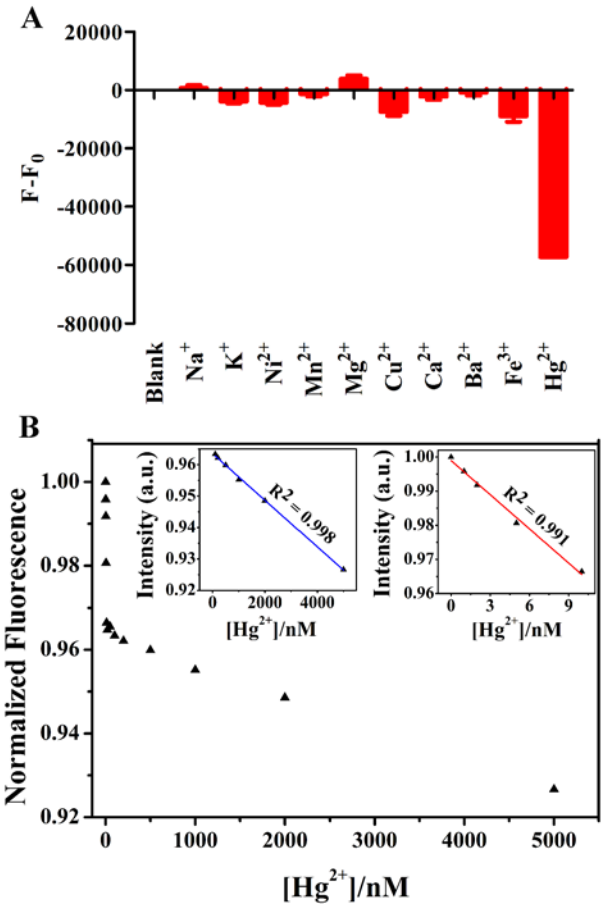

Fig. 6 (A) Influence of different metal ions on the PL intensity of the CDs-1. (B) The sensitivity of Hg^{2+} detection.

4. Conclusions

In summary, we present a novel, efficient and simple synthetic approach for strongly green and yellow fluorescent carbon dots (CDs) using L-valine as carbon source with phosphoric acid as the oxidation agent. The fluorescent colour of carbon dots (CDs) can be feasibly tuned by changing the reaction time under a mild temperature. The obtained green carbon dots (CDs) show a high selectivity and sensitivity for Hg^{2+} detection. Two different fluorescence quenching modes are discovered. The limit of detection (LOD) was about 1.51 nM, which is much lower than what's reported in most of the previous publications.

Acknowledgements

This work was supported by the State Key Project of Fundamental Research (Grants 2014CB931900 and 2012CB932504), "Hundred Talents Project" and Scientific Research Equipment Project of the Chinese Academy of Sciences.

Notes and references

College of Materials Science and Opto-electronic Technology, University of Chinese Academy of Sciences, Beijing 100049, China. Fax: 86-10-88256840; Tel: 86-10-88256840; E-mail: liuxf@ucas.ac.cn (X. Liu); cuiyy@ucas.ac.cn (Y. Cui)

1 S. Jayabal, R. Sathiyamurthi and R. Ramaraj, *J. Mater. Chem. A*, 2014, 2, 8918-8925.
2 R. Z. Zhang and W. Chen, *Biosens. Bioelectron.*, 2014, 55, 83-90.
3 N. Vasimalai and S. A. John, *J. Mater. Chem. A*, 2013, 1, 4475-4482.
4 Y. Si, X. Wang, Y. Li, K. Chen, J. Wang, J. Yu, H. Wang and B. Ding, *J. Mater. Chem. A*, 2014, 2, 645-652.
5 K. Leopold, M. Foulkes and P. Worsfold, *Anal. Chim. Acta*, 2010, 663, 127-138.
6 M. Zhang, L. Ge, S. Ge, M. Yan, J. Yu, J. Huang and S. Liu, *Biosens. Bioelectron.*, 2013, 41, 544-550.
7 Q.-J. Ma, X.-B. Zhang, X.-H. Zhao, Z. Jin, G.-J. Mao, G.-L. Shen and R.-Q. Yu, *Anal. Chim. Acta*, 2010, 663, 85-90.
8 C.-K. Chiang, C.-C. Huang, C.-W. Liu and H.-T. Chang, *Anal. Chem.*, 2008, 80, 3716-3721.
9 X. Yang, Y. Zhuo, S. Zhu, Y. Luo, Y. Feng and Y. Dou, *Biosens. Bioelectron.*, 2014, 60, 292-298.
10 Y. Chen and Z. Rosenzweig, *Anal. Chem.* , 2002, 74, 5132-5138.
11 A. M. Derfus, W. C. W. Chan and S. N. Bhatia, *Nano Lett.*, 2004, 4, 11-18.
12 R. Gill, M. Zayats and I. Willner, *Angew. Chem. Int. Ed.*, 2008, 47, 7602-7625.
13 B. Y. Yu and S.-Y. Kwak, *J. Mater. Chem.*, 2012, 22, 8345-8353.
14 X. Guo, C.-F. Wang, Z.-Y. Yu, L. Chen and S. Chen, *Chem. Commun.*, 2012, 48, 2692-2694.
15 A. Zhu, Q. Qu, X. Shao, B. Kong and Y. Tian, *Angew. Chem.*, 2012, 124, 7297-7301.
16 M. Algarra, M. Perez-Martin, M. Cifuentes-Rueda, J. Jimenez-Jimenez, J. da Silva, T. J. Bandosz, E. Rodriguez-Castellon, J. T. L. Navarrete and J. Casado, *Nanoscale*, 2014, 6, 9071-9077.
17 W. Wei, C. Xu, J. Ren, B. Xu and X. Qu, *Chem. Commun.*, 2012, 48, 1284-1286.
18 L. Zhou, Y. Lin, Z. Huang, J. Ren and X. Qu, *Chem. Commun.*, 2012, 48, 1147-1149.
19 S. Sahu, B. Behera, T. K. Maiti and S. Mohapatra, *Chem. Commun.*, 2012, 48, 8835-8837.
20 Z. Q. Xu, L. Y. Yang, X. Y. Fan, J. C. Jin, J. Mei, W. Peng, F. L. Jiang, Q. Xiao and Y. Liu, *Carbon*, 2014, 66, 351-360.
21 K. Ai, Y. Liu, C. Ruan, L. Lu and G. Lu, *Adv. Mater.*, 2013, 25, 998-1003.
22 Y. Song, W. Shi, W. Chen, X. Li and H. Ma, *J. Mater. Chem.*, 2012, 22, 12568-12573.
23 C. Liu, P. Zhang, X. Zhai, F. Tian, W. Li, J. Yang, Y. Liu, H. Wang, W. Wang and W. Liu, *Biomaterials*, 2012, 33, 3604-3613.
24 H. M. R. Gonçalves, A. J. Duarte and J. C. G. Esteves da Silva, *Biosensors and Bioelectronics*, 2010, 26, 1302-1306.
25 S. N. Baker and G. A. Baker, *Angew. Chem. Int. Ed.*, 2010, 49, 6726-6744.
26 H. Li, Z. Kang, Y. Liu and S.-T. Lee, *J. Mater. Chem.*, 2012, 22, 24230-24253.
27 Y.-L. Zhang, L. Wang, H.-C. Zhang, Y. Liu, H.-Y. Wang, Z.-H. Kang and S.-T. Lee, *RSC Adv.*, 2013, 3, 3733-3738.
28 Q. Wang, H. Zheng, Y. Long, L. Zhang, M. Gao and W. Bai, *Carbon*, 2011, 49, 3134-3140.
29 Y. Dong, H. Pang, H. B. Yang, C. Guo, J. Shao, Y. Chi, C. M. Li and T. Yu, *Angew. Chem. Int. Ed.*, 2013, 52, 7800-7804.
30 H. Liu, T. Ye and C. Mao, *Angew. Chem. Int. Ed.*, 2007, 46, 6473-6475.
31 Z. Ma, H. Ming, H. Huang, Y. Liu and Z. Kang, *New J. Chem.*, 2012, 36, 861-864.
32 J. Zhang, W. Shen, D. Pan, Z. Zhang, Y. Fang and M. Wu, *New J. Chem.*, 2010, 34, 591-593.
33 Y. Yang, J. Cui, M. Zheng, C. Hu, S. Tan, Y. Xiao, Q. Yang and Y. Liu, *Chem. Commun.*, 2012, 48, 380-382.
34 X. Xu, R. Ray, Y. Gu, H. J. Ploehn, L. Gearheart, K. Raker and W. A. Scrivens, *J. Am. Chem. Soc.*, 2004, 126, 12736-12737.
35 Y.-P. Sun, B. Zhou, Y. Lin, W. Wang, K. S. Fernando, P. Pathak, M. J. Meziani, B. A. Harruff, X. Wang and H. Wang, *J. Am. Chem. Soc.*, 2006, 128, 7756-7757.
36 H. Jiang, F. Chen, M. G. Lagally and F. S. Denes, *Langmuir*, 2009, 26, 1991-1995.
37 X. Jia, J. Li and E. Wang, *Nanoscale*, 2012, 4, 5572-5575.
38 H. Li, H. Ming, Y. Liu, H. Yu, X. He, H. Huang, K. Pan, Z. Kang and S.-T. Lee, *New J. Chem.*, 2011, 35, 2666-2670.
39 Y. Li, Y. Zhao, H. Cheng, Y. Hu, G. Shi, L. Dai and L. Qu, *J. Am. Chem. Soc.*, 2011, 134, 15-18.
40 Z. Zhang, J. Zhang, N. Chen and L. Qu, *Energy. Environ. Sci.*, 2012, 5, 8869-8890.
41 W. Wei, C. Xu, L. Wu, J. Wang, J. Ren and X. Qu, *Sci. Rep*, 2014, 4.
42 S. Hu, A. Trinchi, P. Atkin and I. Cole, *Angew. Chem. Int. Ed.*, 2015, 54, 2970-2974.
43 K. Jiang, S. Sun, L. Zhang, Y. Lu, A. Wu, C. Cai and H. Lin, *Angew. Chem. Int. Ed.*, 2015, 54, 1-5.
44 Z. Luo, Y. Lu, L. A. Somers and A. C. Johnson, *J. Am. Chem. Soc.*, 2009, 131, 898-899.
45 Z. Qian, X. Shan, L. Chai, J. Ma, J. Chen and H. Feng, *ACS App. Mater. Inter.*, 2014, 6, 6797-6805.
46 J. Peng, W. Gao, B. K. Gupta, Z. Liu, R. Romero-Aburto, L. Ge, L. Song, L. B. Alemany, X. Zhan, G. Gao, S. A. Vithayathil, B. A. Kaipparettu, A. A. Marti, T. Hayashi, J.-J. Zhu and P. M. Ajayan, *Nano Letters*, 2012, 12, 844-849.
47 H. Ding, P. Zhang, T. Y. Wang, J. L. Kong and H. M. Xiong, *Nanotechnology*, 2014, 25, 1-9.
48 S. K. Bhunia, N. Pradhan and N. R. Jana, *ACS App. Mater. Inter.*, 2014, 6, 7672-7679.
49 X. Dong, Y. Su, H. Geng, Z. Li, C. Yang, X. Li and Y. Zhang, *J. Mater. Chem. C*, 2014, 2, 7477-7481.
50 Y. Liu, N. Xiao, N. Q. Gong, H. Wang, X. Shi, W. Gu and L. Ye, *Carbon*, 2014, 68, 258-264.
51 C. Guo and J. Irudayaraj, *Anal. Chem.* , 2011, 83, 2883-2889.
52 N. Goswami, A. Giri, M. S. Bootharaju, P. L. Xavier, T. Pradeep and S. K. Pal, *Anal. Chem.* , 2011, 83, 9676-9680.
53 H. Goncalves, P. A. S. Jorge, J. R. A. Fernandes and J. C. G. Esteves da Silva, *Sensor. Actuat. B-Chem.*, 2010, 145, 702-707.
54 W. Wang, T. Kim, Z. Yan, G. Zhu, I. Cole, N. Nam-Trung and Q. Li, *J. Colloid Interf. Sci.*, 2015, 437, 28-34.

